

Elastic anisotropy and yield surface estimates of polycrystals

R. Brenner^{a,*}, R.A. Lebensohn^b, O. Castelnau^a

^aLaboratoire des Propriétés Mécaniques et Thermodynamiques des Matériaux, CNRS-UPR9001, Institut Galilée, Université Paris Nord, av. J.B. Clément, 93430 Villetaneuse, France

^bMaterials Science and Technology Division, Los Alamos National Laboratory, Los Alamos, NM 87845, USA

ARTICLE INFO

Article history:

Received 6 December 2008

Received in revised form 10 March 2009

Available online 10 April 2009

Keywords:

Yield surface

Polycrystals

Self-consistent model

Elastic anisotropy

Fast Fourier Transform

ABSTRACT

Homogenization estimates based on the self-consistent scheme are customarily used to describe the plastic yielding of polycrystals. Such estimates of the initial micro yield surface of a polycrystal depend on the morphologic and crystallographic textures, the slip system geometry, the corresponding critical resolved shear stresses and the single crystal elastic anisotropy. The usual approach relies on a rather crude description of the stress field induced by the local elastic anisotropy. This deficiency is addressed and a new concept, i.e. a “probability” yield surface is proposed. Based on a statistical description of the local fields, the latter makes use of the average and the standard deviation of the resolved shear stress on the different slip systems within a given crystalline orientation. By comparing the homogenization estimates with full-field results, it is shown that the self-consistent scheme does not present intrinsic shortcomings regarding the prediction of the micro yield stress of polycrystals with anisotropic elastic constitutive behaviour. On the contrary, it delivers realistic estimates if the local field fluctuations are taken into account in the yield criterion. The quantitative results obtained for cubic elasticity show a strong influence of the intragranular stress heterogeneity on the estimate of the micro yield stress.

© 2009 Elsevier Ltd. All rights reserved.

1. Introduction

The initial yield surface of polycrystals can be defined in various ways. By using an experimental macroscopic stress–strain curve, the *macro yield* stress of a polycrystalline metallic material is customarily determined by considering the stress for an offset plastic strain of 0.2%. It is assumed that all grains have entered the plastic regime when this stress is reached. This conventional definition gives necessarily an upper limit for the yield stress of the polycrystal. By contrast, the *micro yield* stress corresponds to the onset of plastic slip in the polycrystal. The influence of the spatial heterogeneity of elastic properties on the inception of plasticity has been first brought to light qualitatively by slip trace analysis in bicrystals (Hook and Hirth, 1967) and in polycrystals (Hashimoto and Margolin, 1983a). Indeed, these works have reported operating slip systems with low Schmid factors and a preferential slip activity near grain boundaries during the first stage of the elastoplastic transition. As a consequence, an accurate determination of the yield stress of a polycrystal requires the knowledge of the stress field that develops in the material during the linear elastic regime. It should be also noted that the stress field that develops due to elastic interaction between grains has been put forward by some authors to describe the grain size dependence of the yield stress (Meyers and Ashworth, 1982; Margolin et al., 1986). From an experimental point of view, the recent development of microdif-

fraction techniques allows a quantitative investigation of the crystalline lattice distortions at the grain scale (Tamura et al., 2003). This technique can thus be used to detect the onset of plasticity and, more generally, to characterize the local plastic response of polycrystals (Castelnau et al., 2006b; Ungár et al., 2007). Such experimental results can be compared with estimates derived from micromechanical modelling approaches that describe the heterogeneity of the mechanical fields resulting from the microstructural topology and the anisotropy of the local constitutive behaviour. To be more precise, micromechanical estimates of the micro yield stress are functions of the spatial arrangement of grains, the crystallographic texture, the slip system geometry together with the critical resolved shear stresses, and the single crystal elastic moduli. To tackle this problem, two types of micromechanical approaches can be chosen: a *mean-field* modelling (i.e. homogenization theory) which makes use of a statistical description of the microstructure and a *full-field* computation based on a spatial description of the microstructure.

The link between the single crystal elastic anisotropy and the onset of yielding in polycrystals has been first studied within the homogenization framework by Hutchinson (1970) who used the linear elastic self-consistent model (Hershey, 1954; Kröner, 1958) to estimate the micro yield stress. Hutchinson defined the latter as the lowest macroscopic stress required to activate plastic slip within the polycrystal. His self-consistent analysis relied on the average stress field at the grain scale determined by using the Eshelby's inclusion result (Eshelby, 1957). Since then, this model has been widely used to simulate experiments (see, for instance,

* Corresponding author.

E-mail address: rb@galilee.univ-paris13.fr (R. Brenner).

Turner et al., 1995; Clausen et al., 1998; Pang et al., 1999). However, Hutchinson reported that the self-consistent model describes an increase of the plastic yielding onset compared to the isotropic elastic case, whereas elastic heterogeneities are expected to decrease the initial yield point. This feature has been interpreted as a shortcoming of the self-consistent model which was mistakenly believed to deliver an homogeneous stress field within each grain of the polycrystal. Indeed, Hutchinson explained this apparent drawback by stating that "... The reason for this stems from the fact that stresses in each grain are calculated by treating it as a spherical inclusion. Stresses in the matrix surrounding the inclusion do not enter into the self-consistent estimate of initial yield ..." (Hutchinson, 1970). With this remark in mind, one of the purposes of the present paper is to derive new self-consistent estimates of the micro yield stress by making use of the entire available information on the stress fluctuations within the polycrystalline material. To this end, comparisons with corresponding full-field solutions will be instrumental to validate our homogenization analysis.

Numerous works have been devoted to the full-field modeling of the elastic response of locally anisotropic polycrystalline aggregates, in connection with the microplasticity onset. The Finite Element Method (FEM) has been customarily chosen to perform this analysis. Among others, we can cite the early study of Hashimoto and Margolin (1983b) on polycrystalline α -brass with columnar grains, the work of Kumar et al. (1996) who considered a three-dimensional (3-D) Poisson–Voronoi tessellation, and the recent investigations on thin films microstructures (Wikström and Nygards, 2002; Geandier et al., 2008) and fields distribution at free surfaces (Sauzay, 2007; Zeghadi et al., 2007). These different studies clearly evidenced the influence of the elastic heterogeneities on the stress field fluctuations, especially near grain boundaries. It is clear that, beyond the description of the effective behaviour, full-field models provide significant information on local fields. They can thus be used to characterize the local fields distribution and to assess the accuracy of homogenization estimates at *both* macroscopic and local scales. Such comparisons have been performed for viscoplastic polycrystals (Lebensohn et al., 2004), by using a method based on Fast Fourier Transform (FFT) (Moulinec and Suquet, 1998; Lebensohn, 2001), but few detailed studies exist for polycrystal elasticity. This question has been only partially addressed by Yaguchi and Busso (2005) who performed comparisons of the overall elastic properties of columnar microstructures.

In this paper, we first present a thorough analysis of the local fields distribution within a Representative Volume Element (RVE) of an elastic polycrystalline aggregate using, on the one hand, the FFT-based full-field modelling and, on the other hand, the self-consistent scheme (Section 2). Next, the link between the elastic stress field and the definition of the micro yield stress, which constitutes the central issue of this article, is discussed and an original probability approach for the determination of the yield surface is described (Section 3). Using this "probability" yield surface, the accuracy of various self-consistent estimates, including the one given by Hutchinson (1970), is then discussed by comparison with reference full-field results (Section 4).

2. Local fields within elastic polycrystals

Let us consider a RVE with volume Ω of an elastic polycrystalline medium. In what follows, the notion of *representativity* encompasses both mechanical and microstructural definitions. Thus, the volume Ω is said representative if: (i) Hill's macrohomogeneity condition is fulfilled and (ii) all the statistical information on the microstructure is contained in Ω (Hill, 1963). Our study is concerned with polycrystals presenting a random homogeneous and isotropic microstructure. This implies, in particular, equiaxed

grains and a random repartition of the crystalline orientations within the material. Besides, it is assumed that the elastic tensor field $\mathbf{C}(\mathbf{x})$ is ergodic. It is worth noting that the RVE status of such random media has been rigorously justified (Sab, 1992).

2.1. Full-field modelling: FFT-based method

Given a complete description of a polycrystalline microstructure, various numerical methods can be used to compute its mechanical response. Up to now, the FEM remains the most widely used. In this article, we chose to use an alternative method, originally proposed by Moulinec and Suquet (1998), which makes use of the Fourier transform technique to solve the heterogeneous elasticity problem in a periodic unit cell. This method relies on the integral equation for the strain field, also called Lippmann–Schwinger equation (see, for instance, Zeller and Dederichs, 1973). The main attracting features of this numerical scheme are the possibility of using images of the microstructure as direct input (no meshing required) and a low numerical cost (problems with several millions of degrees of freedom (d.o.f.) can be solved in a few minutes without parallel computing, see Appendix B). The reader is referred to Moulinec and Suquet (1998), Eyre and Milton (1999), Michel et al. (2001) for a detailed description of the method and to Lebensohn (2001) who first used it to investigate the local response of elastic and viscoplastic polycrystalline aggregates made of cubic-shaped grains.

2.1.1. Unit cell description

To construct a cubic polycrystalline unit cell of volume Ω_{UC} , a Poisson–Voronoi tessellation has been chosen. Dating from the work of Kumar and Kurtz (1994), this microstructural model is widely used to study the physical properties of equiaxed polycrystalline microstructures because it mimics the homogeneous crystal growth process. Note that in our case periodicity has to be imposed on the microstructure to be consistent with the requirements of the FFT-based method and to avoid artificial boundary effects (see also Nygards and Gudmundson, 2002). This is ensured by the periodic duplication of Voronoi seeds immediately outside the unit cube. A set of 500 initial seeds is used to generate the tessellation and a uniform crystalline orientation is assigned to each resulting Voronoi cell. For that goal, a set \mathcal{N}_φ of 500 crystalline orientations generated with a quasi-random Sobol process has been used. There is thus a one-to-one correspondence between the set of Voronoi cells and the set of crystalline orientations. The obtained cubic unit cell is further discretized into a regular grid consisting of $128 \times 128 \times 128$ voxels (Fig. 1a). Each grain thus comprises 4200 voxels on average. The set of orientations \mathcal{N}_φ and the Voronoi tessellation process lead to a quasi-isotropic Orientation Distribution Function (ODF). Consequently, the volumetric average of the elastic tensor field over an unique unit cell is quasi-isotropic and can be considered as a good approximation of its ensemble average (i.e. 1-point correlation function) over the set of equiprobable realizations \mathcal{P}_z . It can thus be concluded that a polycrystalline unit cell of volume Ω_{UC} is isotropic of grade 1 following Kröner's terminology (Kröner, 1977). By contrast, for grade $n > 1$, the volumetric average over Ω_{UC} does not *a priori* identify with the n -point correlation function and it follows that the ergodicity assumption is not verified by Ω_{UC} . Consequently, the constructed unit cell is *not* a RVE. In particular, it does not contain several grains with the same crystalline orientation but different neighbouring environments.

2.1.2. Approximation of the RVE's response

To approximate the RVE's response of a polycrystal, we apply the procedure of ensemble averaging (see, for instance, Sab, 1992). Let α be a particular realization in the set \mathcal{P}_z of equiprobable realizations (i.e. the set of cubic unit cells generated by Poisson–

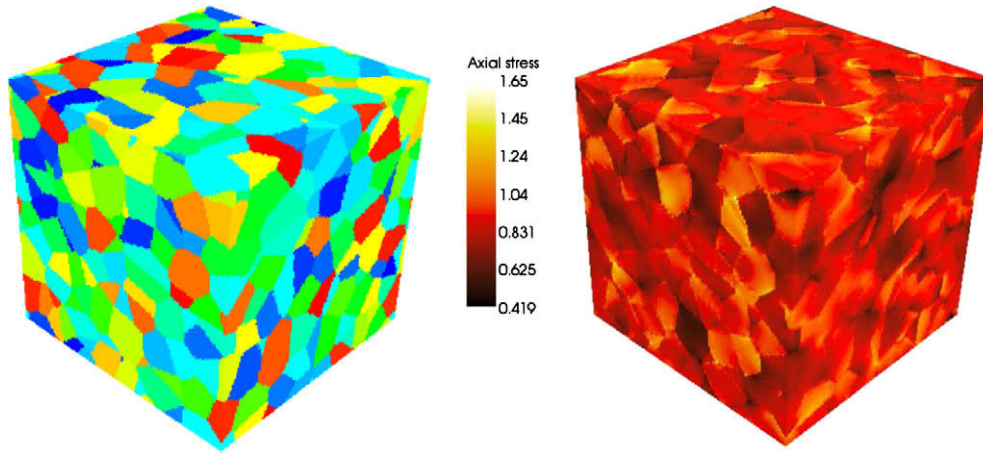


Fig. 1. Periodic Poisson–Voronoi tessellation containing 500 grains with uniform crystalline orientations (a) and corresponding axial stress field for a tensile loading (b).

Voronoi tessellation) and let t be a random field, statistically homogeneous and ergodic. Then, the expectation of t defined by $\langle t \rangle^{\mathcal{P}_\alpha} = \int_{\mathcal{P}_\alpha} t(\alpha) d\alpha$ can be approximated by a Monte–Carlo computation

$$\langle t \rangle^{\mathcal{P}_\alpha} \approx \frac{1}{N_\alpha} \sum_{i=1}^{N_\alpha} t(\alpha_i) \quad (1)$$

with N_α being the number of unit cell realizations. The ergodicity assumption implies that the expectation of t is equal to the volumic average of t over Ω . Note that the generation of different unit cells is performed with the fixed set of orientations \mathcal{N}_φ and randomly varying Voronoi seeds positions. Grains with the same crystalline orientation but varying neighbourhoods are thus present in the different realizations. This allows us to also perform rigorous ensemble averages of the mechanical fields per crystalline orientation.

2.1.3. Fields description

An important aspect of the present analysis is to assess the accuracy of the ensemble averaging procedure at different scales. In order to perform ensemble averages, we have generated 100 unit cell realizations and considered the local constitutive elastic behaviour of a crystal with cubic lattice symmetry. The anisotropy of the local elastic behaviour can be characterized by the parameter A introduced by Zener (1948), which reads, using standard Voigt notation: $A = 2C_{44}/(C_{11} - C_{12})$. Each unit cell has been subjected to uniaxial tensile, simple shear and mixed tensile–shear loadings. For illustration, the axial stress field distribution, normalized by the corresponding macroscopic value, for a tensile loading and anisotropy parameter $A = 2.8$ is shown in Fig. 1b. As expected, strong fluctuations of the local axial stress are obtained, with maxima appearing preferentially close to grain boundaries and a stress concentration factor varying between 0.4 and 1.6 for this particular unit cell.

While some results have been reported in the literature on the size of the RVE necessary to estimate the effective properties of polycrystalline materials within a given error (see, e.g. Nygard, 2003; Houdaigui et al., 2007), in the present investigation we analyze the representativity of our results at both macroscopic and local scales (“local” refers here to the scale of individual crystals). According to sampling theory, the relative error on the expectation of an homogeneous and ergodic random variable t is expressed as

$$\epsilon_t = \frac{2SD^{\mathcal{P}_\alpha}(t)}{\langle t \rangle^{\mathcal{P}_\alpha} \sqrt{N_\alpha}} \quad (2)$$

where the standard deviation $SD^{\mathcal{P}_\alpha}(t)$ and the average $\langle t \rangle^{\mathcal{P}_\alpha}$ are approximated by a Monte–Carlo computation of the ensemble aver-

age on N_α realizations (1). The error ϵ_t is thus important when the random variable t strongly vary from one realization to another. To quantify the accuracy of the full-field results at different scales, we have considered three random variables: the overall equivalent stress $\bar{\sigma}_{\text{eq}}$, the equivalent of the average stress $\langle \sigma \rangle_{\text{eq}}^r$ and the standard deviation of the equivalent stress $SD^r(\sigma_{\text{eq}})$ within a given grain orientation which has been arbitrarily chosen in the set \mathcal{N}_φ . The evolution of the sampling error for each variable with respect to the number of realizations N_α is reported on Fig. 2, for Zener parameter $A = 2.8$, in the case of a tensile loading. As expected, a decrease of the error ϵ is obtained with the increase of N_α . It is worth mentioning that the minimum attainable error depends on the local anisotropy, the discretization and the size of the unit cell. In the studied case, we obtain a relative error of 0.1% on the macroscopic stress, 1% on the average stress per grain orientation and 5% on the standard deviation of the stress within a grain orientation for 100 realizations. There is thus one to two orders of magnitude between the precisions at the overall and local scales for the chosen local description of the stress field. This result can be explained by the fact that the overall stress depends at first order on the 1-point correlation function of the elastic tensor field which slightly varies from one realization to another. By contrast, the average and standard deviation of the local stress within a grain with a given crystalline orientation is strongly affected by its neighbourhood (i.e. by higher-order correlation functions of the elastic tensor field). This results in less accurate estimates of the local fields compared to

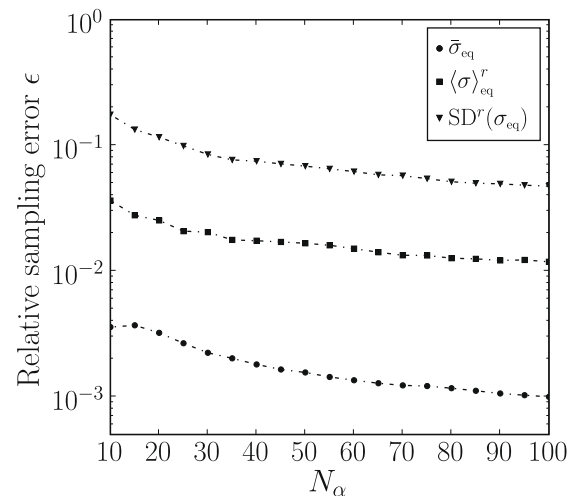


Fig. 2. Relative sampling error of the stress field at different scales vs. the number of unit-cell realizations.

the macroscopic fields, for a given number of realizations. The effect of the neighbouring grains on the local stress field can be further illustrated by investigating the stress distributions. Fig. 3 shows the effect of the number of realizations on the shape of the distribution within a given crystalline orientation. For a single realization, the stress distribution within a single crystalline orientation is far from Gaussian, but it gets closer to Gaussian when many random realizations are considered although there is no proof that it becomes really Gaussian. The addition of different grain environments thus tends to smooth out the local stress field distribution. It is emphasized that this distribution is expected to be a good approximation of the one that would have been obtained if we had considered a polycrystalline volume element containing grains with the same crystalline orientation but randomly located in the specimen as in Castelnau et al. (2006a). On the other hand, it can be observed that the stress field distribution in the whole sample is already almost symmetric for a single unit cell (Fig. 3). It should be mentioned that field distributions close to Gaussian have previously been reported in two-dimensional linear composites with “particulate” (i.e. matrix–inclusion) microstructure (Moulinec and Suquet, 2003).

2.2. Mean-field modelling: self-consistent scheme

By contrast with the previous full-field numerical approach, mean-field estimates (a.k.a homogenization estimates) rely on an incomplete statistical description of the microstructure. In the case of polycrystals, the heterogeneity is related to the existence of different crystalline orientations or *mechanical phases*. Each mechanical phase r has a volume Ω_r , and its spatial repartition is described by the characteristic function $\chi^r(\mathbf{x})$, which is equal to 1 if $\mathbf{x} \in \Omega_r$ and 0 otherwise. An elastic polycrystal can be considered to be a composite material made of N crystalline orientations such that

$$\mathbf{C}(\mathbf{x}) = \sum_{r=1}^N \mathbf{C}^r \chi^r(\mathbf{x}) \quad (3)$$

where \mathbf{C}^r is the elastic moduli tensor of mechanical phase r . The microstructure of the polycrystalline material is statistically described by the n -point correlation functions of the characteristic functions. Due to the “granular” character of a polycrystal (i.e. all crystalline orientations are on the same footing), the self-consistent model (Hershey, 1954) is expected to be well adapted for this kind of microstructures (see Kröner, 1978). It is recalled that, in a homogenization context, the localization problem linking the local

strain field $\boldsymbol{\varepsilon}(\mathbf{x})$ to the overall strain $\bar{\boldsymbol{\varepsilon}}$ cannot be solved. Nevertheless, using the statistical description of the microstructure and the uniformity per phase of the local behaviour, the problem can be degenerated by considering only the average localization for each crystalline orientation.

2.2.1. Self-consistent estimate

By considering ellipsoidal 2-point correlation functions (Willis, 1977), the estimate of the effective elastic tensor $\tilde{\mathbf{C}}$ can be derived using Eshelby’s solution (Eshelby, 1957) for an ellipsoidal inclusion embedded in an infinite homogeneous linear medium, itself subjected to an homogeneous loading. The self-consistent estimate of $\tilde{\mathbf{C}}$ reads

$$(\tilde{\mathbf{C}} + \mathbf{C}^*)^{-1} = \langle (\mathbf{C} + \mathbf{C}^*)^{-1} \rangle \quad (4)$$

where $\mathbf{C}^* = \mathbf{P}^{-1} - \tilde{\mathbf{C}}$ is the “constraint” tensor which reflects the reaction of the homogeneous medium to the deformation of the inclusion. It depends on the Hill tensor \mathbf{P} which is a function of the elastic properties of the effective medium and the shape of the inclusion (see Appendix A).

At the local scale, the self-consistent model delivers information about the average fields per crystalline orientation. For instance, the local average strain tensor reads

$$\langle \boldsymbol{\varepsilon} \rangle^r = (\mathbf{C}^r + \mathbf{C}^*)^{-1} : (\tilde{\mathbf{C}} + \mathbf{C}^*) : \bar{\boldsymbol{\varepsilon}} \quad (5)$$

The local average stress tensor can be obtained using the constitutive relation: $\langle \boldsymbol{\sigma} \rangle^r = \mathbf{C}^r : \langle \boldsymbol{\varepsilon} \rangle^r$. However, the statistical description of the local stress and strain fields is not limited in the mean-field framework to this first-order information. Indeed, the homogenization procedure also delivers estimates of the field fluctuations. More precisely, the second moment of the intraphase field distribution can be obtained by considering partial derivatives of the effective elastic energy with respect to the local elastic behaviour (see Bergman, 1978; Bobeth and Diener, 1987; Kreher, 1990; Ponte Castañeda and Suquet, 1998). This result follows from the quadratic dependence of the elastic energy on the stress and strain fields. For instance, the intraphase second moment of the strain field for crystalline orientation r is given by

$$\langle \boldsymbol{\varepsilon} \otimes \boldsymbol{\varepsilon} \rangle_{ijkl}^r = \frac{1}{c_r} \bar{\boldsymbol{\varepsilon}} : \frac{\partial \tilde{\mathbf{C}}}{\partial \mathbf{C}_{ijkl}^r} : \bar{\boldsymbol{\varepsilon}}. \quad (6)$$

Its explicit computation, in a general anisotropy context, is given in Appendix A.

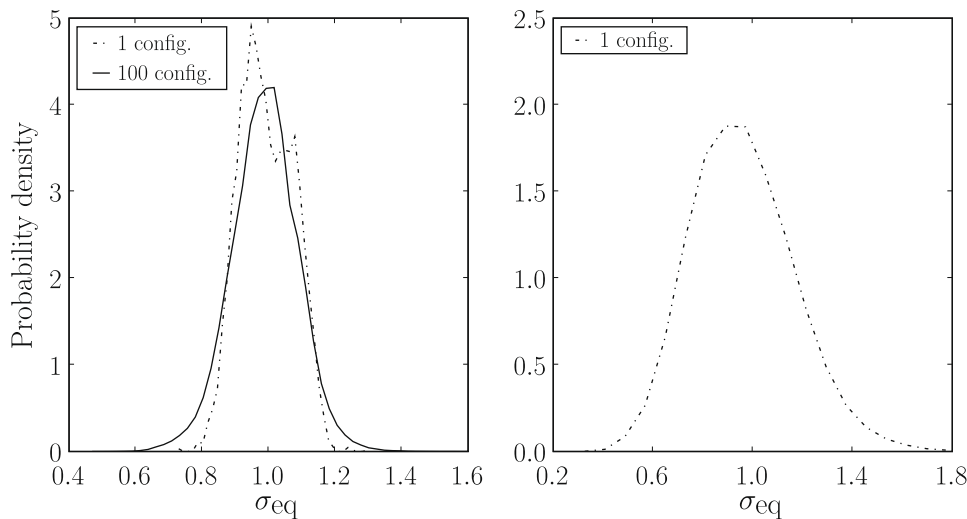


Fig. 3. Normalized equivalent stress field distribution within a single crystalline orientation (left) and within the whole unit cell (right). Note that a similar distribution is obtained with 100 configurations for the whole unit cell.

2.2.2. Fields description

The self-consistent estimate of the elastic response of the polycrystalline RVE has been computed numerically. In doing this, we have considered a spherical shape for the covariances and the above-described set \mathcal{N}_ϕ of crystalline orientations with equal weights. The implicit self-consistent Eq. (4) has been solved iteratively with a relative error of 10^{-6} . The good agreement between the FFT-based computations and the linear self-consistent estimate has been previously reported for different polycrystalline microstructures, namely: 2-D Voronoi tessellations (Castelnau et al., 2006a) and 3-D polycrystals with cubic grains (Lebensohn et al., 2004), and was expected to also hold in the present 3-D Voronoi case. Indeed, a relative error of about 1% is obtained on the average and second moment of the stress and strain distributions within each crystalline orientation. This is the minimum error that could be achieved since it is of the same order as the sampling error on the intragranular average and standard deviation of the stress field, as already discussed (Fig. 2).

3. Yield surface estimates

The results of the previous section highlight the strong stress heterogeneity induced in a polycrystalline RVE made of grains with local elastic anisotropy. Moreover, the pertinence of the self-consistent scheme to describe the stress field distribution for linear polycrystal has been demonstrated by comparison with full-field computations. Based on these results, the way in which this available statistical information can be used to accurately describe the onset of plasticity in a polycrystal is now addressed.

3.1. Shortcoming of previous mean-field estimates

As discussed previously, Hutchinson (1970) was the first to shed light on the influence of the local elastic anisotropy on the micro yield stress estimated by means of the self-consistent scheme. Indeed, earlier assessments of the self-consistent model for elastoplastic polycrystals relied on a simplifying assumption of elastic isotropy (Budiansky et al., 1960; Kröner, 1961). Hutchinson's analysis focused on the self-consistent prediction of the initial yield surface of a random polycrystal made of FCC single crystals. For this crystalline symmetry, the slip set \mathcal{K} comprises 12 crystallographically equivalent slip systems $\{111\}\{1\bar{1}0\}$. By adopting a description of the local stress field limited to its intraphase mean values, he showed that the self-consistent scheme leads to a modified Tresca criterion, with a yield function f_Y of the form

$$f_Y(\bar{\sigma}) = \max_{I,J} \frac{|\bar{\sigma}_I - \bar{\sigma}_J|}{2} - \tilde{\tau}_0 \quad (7)$$

where $\sigma_i (i=1,2,3)$ are the macroscopic principal stresses. The effective yield stress $\tilde{\tau}_0$ is given by Hutchinson (1970)

$$\tilde{\tau}_0 = \tau_0 \sqrt{\frac{3}{2a^2 + b^2}} \quad (8)$$

where the coefficients a and b are

$$a = \frac{C_{11} - C_{12}}{2\tilde{\mu}(1 - \beta) + \beta(C_{11} - C_{12})}, \quad b = \frac{C_{44}}{\tilde{\mu}(1 - \beta) + \beta C_{44}}, \quad (9)$$

$$\beta = \frac{6}{5} \left(\frac{\tilde{\kappa} + 2\tilde{\mu}}{3\tilde{\kappa} + 4\tilde{\mu}} \right)$$

with $\tilde{\kappa}$ and $\tilde{\mu}$ being the self-consistent estimates of the effective bulk and shear moduli. For cubic polycrystals, it is well-known that the effective bulk modulus coincides with the bulk modulus of the crystallites (Hill, 1952; Mendelson, 1981) whereas the self-consis-

tent overall shear modulus is the positive root of the following cubic equation (Hershey, 1954; Kröner, 1958)

$$8\tilde{\mu}^3 + (5C_{11} + 4C_{12})\tilde{\mu}^2 - C_{44}(7C_{11} - 4C_{12})\tilde{\mu} - C_{44}(C_{11} - C_{12})(C_{11} + 2C_{12}) = 0. \quad (10)$$

For an isotropic local elastic behaviour (i.e. leading to a uniform stress field within the polycrystal), relation (8) gives $\tilde{\tau}_0 = \tau_0$ so that the yield function (7) reduces to the Tresca yield surface (Hill, 1967).

To highlight the influence of the elastic anisotropy on the stress heterogeneity, we have considered different values of the Zener anisotropy parameter. The equivalent stress distribution within the RVE for a tensile loading are reported on Fig. 4. In the case $A = 1$ (i.e. elastic isotropy), the distribution is a Dirac delta function since the polycrystal is homogeneous. An increase of the local anisotropy leads to a spread and a shift of the peak to larger stress values. Similar observations have been made previously in a non-linear context for viscoplastic polycrystals with highly anisotropic grains (see, for instance, Castelnau et al., 2008). Fig. 4 illustrates that an increase of the local anisotropy implies an increase of the stress heterogeneity, which in turn should induce an early plastic yielding of the polycrystal, compared to the isotropic elasticity case (i.e. Tresca yield surface). On the contrary, Hutchinson (1970) observed that the expression of the effective yield stress (Eq. 8) predicts a delayed plastic yielding for a Zener elastic anisotropy parameter A greater than 1 (which is the case of many common metals: Cu, Fe, Al, Ni, ...). Up to now, this apparent deficiency of the self-consistent model has not been addressed.

3.2. New statistical yield criterion incorporating field fluctuations

In order to improve the self-consistent estimate of yielding, we propose to take into account the available information on local stress fluctuations. First, we consider a RVE for which the microstructure is perfectly known. The local Resolved Shear Stress (RSS) on a slip system k , at a given point \mathbf{x}^g of the grid, can be obtained as

$$\tau_k(\mathbf{x}^g) = \boldsymbol{\sigma}(\mathbf{x}^g) : \sum_{r=1}^N \boldsymbol{\mu}_k^r \boldsymbol{\gamma}^r(\mathbf{x}^g) \quad (11)$$

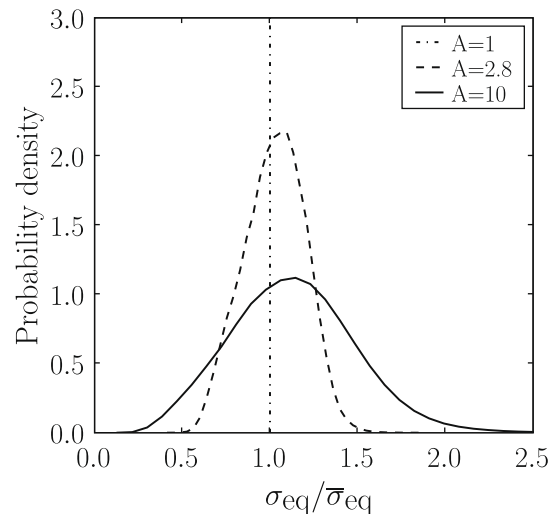


Fig. 4. Distribution of the equivalent stress field distribution within a polycrystalline RVE, for different values of the Zener parameter A , as obtained by the full-field approach.

where μ_k^r is the Schmid tensor of slip system k within crystalline orientation r . According to the Schmid criterion, plasticity occurs when the following condition is fulfilled

$$\max_{\mathbf{x}^g \in \Omega} \max_{k \in \mathcal{K}} |\tau_k(\mathbf{x}^g)| = \tau_0. \quad (12)$$

Although it appears to be a quite straightforward approach to describe the micro yield stress of the polycrystal, this definition presents some important drawbacks. Indeed, it is dependent on the refinement of the grid used for the full-field numerical resolution and, because of the random character of the microstructure, it leads to a yield stress estimate that strongly vary from one unit cell to another. This prevents the use of this criterion to get an accurate estimate of the onset of plasticity.

An alternative approach to define the micro yield stress is making use of the field statistics information. Obviously, different estimates of the onset of plasticity can be obtained, depending on the order of the statistical parameters involved in the yield criterion. For example, Hutchinson (1970) made a very specific choice, disregarding the intraphase stress heterogeneity, defining that yielding of the polycrystal occurs when

$$\max_{r \in \mathcal{N}_\phi} \max_{k \in \mathcal{K}} \langle \tau_k \rangle^r = \tau_0 \quad (13)$$

where \mathcal{N}_ϕ is the finite set of crystalline orientations chosen to represent the crystallographic texture of the polycrystal and $\langle \tau_k \rangle^r = \mu_k^r : \langle \sigma \rangle^r$. We propose a more flexible and general definition of the plastic onset that reads

$$\max_{r \in \mathcal{N}_\phi} \max_{k \in \mathcal{K}} \hat{\tau}_k^r = \tau_0 \quad (14)$$

where $\hat{\tau}_k^r$ is a Reference Resolved Shear Stress (RRSS) that needs to be specified in the general case of a nonuniform intraphase stress field. Based on the information on the local fields that can be obtained with homogenization theory, we propose the following expression

$$\hat{\tau}_k^r = |\langle \tau_k \rangle^r| + pSD^r(\tau_k) \quad (15)$$

which involves the mean value $\langle \tau_k \rangle^r$ and the standard deviation $SD^r(\tau_k)$ of the RSS on slip system k of crystalline orientation r . The latter is given by

$$SD^r(\tau_k) = \sqrt{\langle \tau_k^2 \rangle^r - (\langle \tau_k \rangle^r)^2} \quad \text{with} \quad \langle \tau_k^2 \rangle^r = \mu_k^r : \langle \sigma \otimes \sigma \rangle^r : \mu_k^r. \quad (16)$$

Depending on the value of the positive parameter p , relation (15) leads to different estimates of the initial yield stress of the polycrystal. These estimates can be evaluated for different applied loadings by using the self-consistent scheme or the full-field numerical scheme to determine a so-called *probability yield surface*. This terminology has been chosen by analogy with the notion of confidence intervals in statistics, which indicate the probability of a measurement falling within p standard deviations of the mean (e.g. for a Gaussian distribution, this probability is equal to 0.683 for $p = 1$ and 0.997 for $p = 3$). In the present context, this probability is related to the stress heterogeneity accounted for by the new yield criterion. The value of p parameter can also be related to a more intuitive quantity, i.e. a threshold volume fraction of the grain where plasticity initiates that needs to be in yielding condition to consider that the polycrystal is at the onset of plasticity. This threshold volume fraction decreases as p increases (e.g. if the field distributions in the grains are strictly Gaussians, $p = 1$ amounts to consider that 15.85% of the first plastifying grain has to yield, while for $p = 3$ only a tiny 0.15% volume fraction has to be deforming plastically, to consider that the polycrystal has reached the plasticity onset. Note that the previous estimate of Hutchinson (1970) corresponds to a threshold volume fraction of 50%).

4. Results and discussion

The probability yield criterion (14) and (15) is now applied to the class of polycrystals discussed in Section 2 and its main features are compared to previous works.

First, the accuracy of our self-consistent estimates have been assessed by confrontation with the FFT results. For that goal, sections of the yield surface in the “tension–torsion” plane have been computed, for several assumed p values, using expression (15). Self-consistent calculations were performed with 5° steps while FFT computations were carried out for three particular loading directions: uniaxial tension, pure torsion and a mixed “tension–torsion” loading (Fig. 5) (In the case $p = 0$, the self-consistent numerical computations have been also compared with the analytic solution (8), showing a very good agreement, with a relative discrepancy of about 10^{-3} , likely to be linked to the finite set of crystalline orientations used to approximate an isotropic crystallographic texture.) A very good agreement is obtained between the FFT-based and the self-consistent yield surfaces, for any p value. This is a direct con-

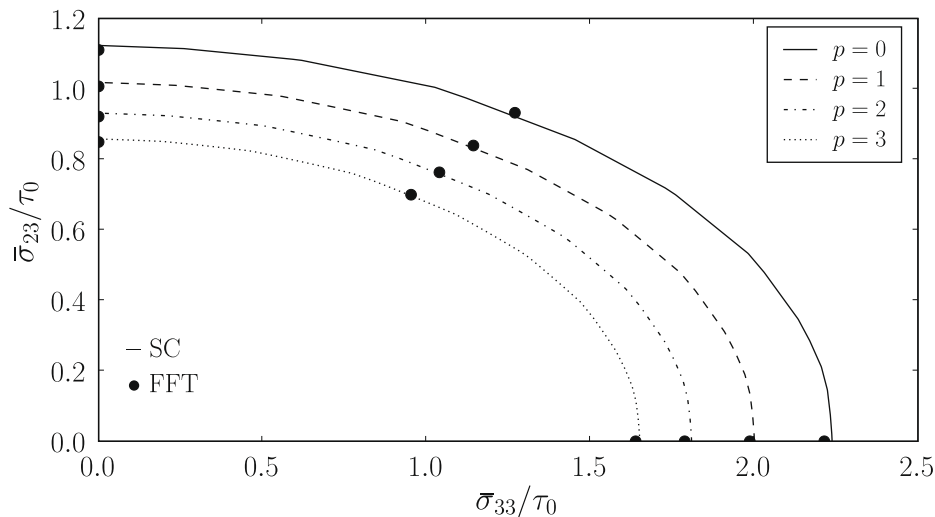


Fig. 5. Self-consistent estimates of yield surface sections obtained with different p values for tension–torsion loadings (curves). FFT estimates are reported for three different loading paths (symbols).

sequence of the excellent agreement between first and second moments of the field distributions within different crystalline orientations computed with both approaches. An important conclusion is thus that the self-consistent model does not present intrinsic drawback concerning the description of the micro yield stress. The shortcoming of Hutchinson's estimate appears to be uniquely related to the choice of the RRSS in the yield criterion (i.e. $\hat{\tau}_k^r = \langle \tau_k \rangle^r$). It is observed that earlier plastic onsets can be predicted when stress heterogeneity enters the yield criterion ($p > 0$). Note also that the yield surfaces remain convex for any p value.

Second, we investigated the physical relevance of the new estimates by computing the evolution of the tensile yield stress for various Zener anisotropy parameters A . In Fig. 6, results are reported for different p values as well as the Tresca yield stress ($\sigma_Y/\tau_0 = 2$). Drastically different variations of the yield stress with the local anisotropy are obtained. For $p = 0$, the self-consistent scheme predicts an increase of the yield stress with respect to the isotropic elastic case, for whatever value of the Zener parameter. This result is in strong disagreement with the stress fluctuations that develop in the polycrystal when the local anisotropy increases (Fig. 4). By contrast, when the intragranular stress heterogeneity is used to define the RRSS ($p > 0$), the yield stress remains

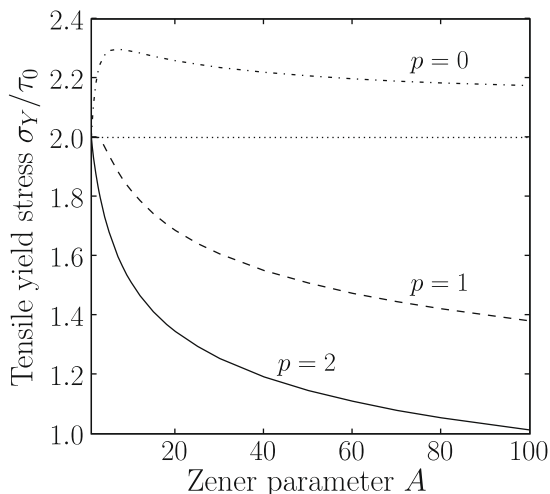


Fig. 6. Self-consistent estimates of the tensile yield stress as a function of the Zener parameter A . Note that the case $p = 0$ corresponds to Hutchinson's estimate. The horizontal dotted line indicates the value of the Tresca yield stress.

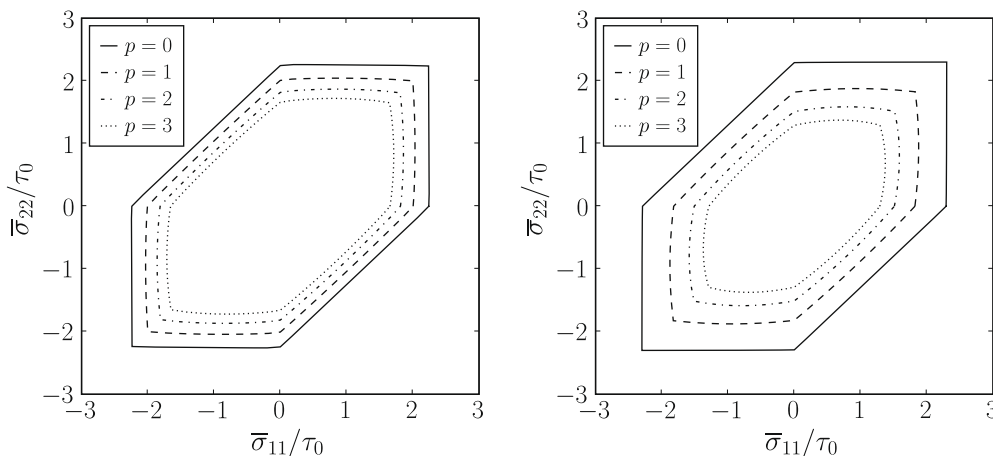


Fig. 7. Self-consistent estimates of yield surface sections obtained with different p values for biaxial loadings. $A = 2.8$ (left) and $A = 10$ (right).

below the Tresca limit and decreases monotonically when A increases. Such behaviour is consistent with an increasing heterogeneity as anisotropy increases.

In what follows, the influence of the field heterogeneity on the shape of the yield criterion is addressed. A section of the yield surface in the $(\bar{\sigma}_{11}, \bar{\sigma}_{22})$ plane is reported in Fig. 7 for two values of the Zener parameter. When $p = 0$, Hutchinson (1970) showed that the "classical" self-consistent scheme determines a *modified* Tresca condition, i.e. the yield surface is obtained by dilation of the Tresca yield surface and thus remains a hexagon in such projection. When the stress heterogeneity is considered in the yield criterion, this is no longer the case. Indeed, our results show that the yield surface departs from a Tresca-type condition. It can be observed that the initially straight segments of the yield surface become curved when stress fluctuations are considered. This deviation from the Tresca-type yield surface is more pronounced for increasing values of parameters A and p . These results indicate that, in general, the initial yield surface of macroscopically isotropic elastoplastic polycrystals does not obey a Tresca-type criterion (7).

5. Concluding remarks

This study sheds light on the effects of the local elastic anisotropy on the onset of plasticity of polycrystalline materials. Our attention has been focused on the description of yielding that can be obtained by means of homogenization theories. Based on a statistical description of local fields and the Schmid criterion, it has been shown that there is not an unique definition of the initial yielding of elastoplastic polycrystals, unless elasticity is isotropic. The definition based on the absolute maximum resolved shear stress in the RVE is useless since this extreme value cannot be determined, except maybe for very specific microstructures for which the complete stress field can be solved analytically. We have proposed an original definition of the initial yield criterion based on field statistics. This new approach defines a set of "probability" yield surfaces. These latter can be associated to threshold volume fractions of the first plastic grain that needs to be in yielding condition. Addressing Hutchinson's remark on an apparent shortcoming of the self-consistent scheme, it has been demonstrated that the incorporation of field fluctuations in the yield criterion leads to physically meaningful self-consistent estimates. In particular, an earlier plastic initiation compared with the elastically isotropic case is predicted and a monotonic decrease of the yield stress estimate is obtained when the stress fluctuations increase. The self-consistent estimates have been successfully compared with the results of full-field computations performed on 3-D polycrystalline

microstructures. Concerning the shape of the yield surface, our investigation highlights the fact that the new “probability” yield surface does not generally follow a Tresca-type criterion. A detailed investigation of the relation between the field fluctuations and the shape of the yield surface, as well as the extension of the present statistical approach to describe the evolution with strain of the yield surface will be subjects of future work. Finally, it is mentioned that the proposed approach might open interesting perspectives for related problems, such as twinning activation in low-symmetry crystalline structures, stress-assisted phase transformation, brittle fracture criterion in polycrystalline ceramics etc. In all these problems, the local stresses distribution plays a critical role and should be taken into account.

Appendix A. Computation of intraphase second moments of stress and strain fields

The numerical computation of the intraphase stress second moment for the self-consistent model has been discussed previously in Brenner et al. (2004). It must be noted that the expressions obtained in this article require symmetrization but this had no consequences on the published results. In this appendix, we derive the concise dual expression for the intraphase strain second moment.

The intraphase stress and strain second moments are linked by the local constitutive elastic law

$$\langle \sigma \otimes \sigma \rangle^r = \mathbf{C}^r : \langle \varepsilon \otimes \varepsilon \rangle^r : \mathbf{C}^r. \quad (\text{A.1})$$

An estimate of the strain second moment can be obtained via the relation

$$\langle \varepsilon \otimes \varepsilon \rangle_{ijkl}^r = \frac{1}{c_r} \bar{\varepsilon} : \frac{\partial \tilde{\mathbf{C}}}{\partial \mathbf{C}_{ijkl}^r} : \bar{\varepsilon} \quad (\text{A.2})$$

A detailed proof of the above relation can be found, in e.g. (Ponte Castañeda and Suquet, 1998).

A.1. Computation of $\partial \tilde{\mathbf{C}} / \partial \mathbf{C}_{ijkl}^r$

The partial derivatives of the self-consistent Eq. (4) with respect to local elastic moduli reads

$$\tilde{\mathbf{F}} : \frac{\partial (\tilde{\mathbf{C}} + \mathbf{C}^*)}{\partial \mathbf{C}_{ijkl}^r} : \tilde{\mathbf{F}} - \left\langle \mathbf{F} : \frac{\partial \mathbf{C}^*}{\partial \mathbf{C}_{ijkl}^r} : \mathbf{F} \right\rangle = \left\langle \mathbf{F} : \frac{\partial \mathbf{C}}{\partial \mathbf{C}_{ijkl}^r} : \mathbf{F} \right\rangle \quad (\text{A.3})$$

with $\tilde{\mathbf{F}} = (\tilde{\mathbf{C}} + \mathbf{C}^*)^{-1}$ and $\mathbf{F} = (\mathbf{C} + \mathbf{C}^*)^{-1}$. The latter is a linear system of equations for the determination of $\partial \tilde{\mathbf{C}} / \partial \mathbf{C}_{ijkl}^r$. Using Kelvin’s convention to represent symmetric fourth order tensors in three dimensions by symmetric second order tensors in six dimensions (Mehrabadi and Cowin, 1990), the latter equation is expressible in the form

$$\Delta_{IJKL} \frac{\partial \tilde{C}_{KL}}{\partial C_{PQ}^r} = \Phi_{IJ}^{r,PQ} \quad (\text{A.4})$$

with

$$\begin{aligned} \Delta_{IJKL} &= \tilde{F}_{IK} \tilde{F}_{LJ} + \tilde{F}_{IM} Q_{MNKL} \tilde{F}_{NJ} - \sum_{s=1}^N c_s F_{IM}^s Q_{MNKL} F_{NJ}^s, \\ Q_{MNKL} &= -P_{MS}^{-1} \frac{\partial P_{ST}}{\partial C_{KL}} P_{TN}^{-1} - \delta_{MK} \delta_{NL}, \\ \Phi_{IJ}^{r,PQ} &= \frac{1}{2} (F_{IP}^r F_{QJ}^r + F_{IQ}^r F_{PJ}^r), \end{aligned} \quad (\text{A.5})$$

where uppercase indices vary between 1 and 6. The estimation of the intraphase second moment of the strain field thus requires the evaluation of the Hill tensor \mathbf{P} and its derivatives $\partial \mathbf{P} / \partial \tilde{\mathbf{C}}_{ijkl}$. In

a general context of elastic anisotropy, these two quantities have to be computed numerically.

A.2. Computation of \mathbf{P} and $\partial \mathbf{P} / \partial \tilde{\mathbf{C}}_{ijkl}$

The Hill tensor \mathbf{P} is defined by a surface integral on the unitary sphere

$$\mathbf{P} = \frac{1}{4\pi |\mathbf{Z}|} \int_{|\xi|=1} \Gamma(\xi) |\mathbf{Z}^{-1} \cdot \xi|^{-3} dS \quad (\text{A.6})$$

where \mathbf{Z} is a second-order tensor defining the assumed ellipsoidal shape of the two-point correlation function of each phase. The Green operator $\Gamma(\xi)$ reads

$$\Gamma = [\xi \otimes \kappa^{-1} \otimes \xi]^{(s)} \quad (\text{A.7})$$

with the acoustic (Christoffel) tensor $\kappa = \xi \cdot \tilde{\mathbf{C}} \cdot \xi$. $[\]^{(s)}$ indicates the (double) minor symmetrization.

The computation of partial derivatives of the Hill tensor thus requires the evaluation of

$$\frac{\partial \Gamma}{\partial \tilde{\mathbf{C}}_{ijkl}} = \left[\xi \otimes \frac{\partial \kappa^{-1}}{\partial \tilde{\mathbf{C}}_{ijkl}} \otimes \xi \right]^{(s)} \quad (\text{A.8})$$

with

$$\frac{\partial \kappa^{-1}}{\partial \tilde{\mathbf{C}}_{ijkl}} = -\kappa^{-1} \cdot \frac{\partial \kappa}{\partial \tilde{\mathbf{C}}_{ijkl}} \cdot \kappa^{-1} = -\kappa^{-1} \cdot \left(\xi \cdot \frac{\partial \tilde{\mathbf{C}}}{\partial \tilde{\mathbf{C}}_{ijkl}} \cdot \xi \right) \kappa^{-1}. \quad (\text{A.9})$$

Taking into account the symmetries of the effective elastic moduli tensor, its derivatives read

$$\begin{aligned} \frac{\partial \tilde{\mathbf{C}}_{mnpq}}{\partial \tilde{\mathbf{C}}_{ijkl}} &= \frac{1}{8} (\delta_{mi} \delta_{nj} \delta_{pk} \delta_{ql} + \delta_{ni} \delta_{mj} \delta_{pk} \delta_{ql} + \delta_{mi} \delta_{nj} \delta_{qk} \delta_{pl} + \delta_{ni} \delta_{mj} \delta_{qk} \delta_{pl} \\ &\quad + \delta_{pi} \delta_{qj} \delta_{mk} \delta_{nl} + \delta_{qi} \delta_{pj} \delta_{mk} \delta_{nl} + \delta_{pi} \delta_{qj} \delta_{nk} \delta_{ml} + \delta_{qi} \delta_{pj} \delta_{nk} \delta_{ml}). \end{aligned}$$

The Hill tensor and its partial derivatives have been computed numerically using Gauss quadrature.

Appendix B. Details on the full-field FFT implementation

The FFT full-field modelling has been implemented using the original scheme of Moulinec and Suquet (1998) since the studied material (i.e. an elastic polycrystal) presents a moderate contrast

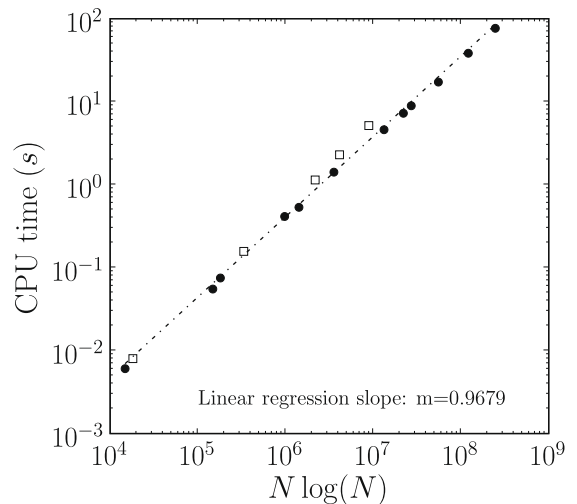


Fig. 8. CPU time per elastic FFT iteration as a function of the number of voxels N . The white squares correspond to unit-cell discretizations with prime numbers in each direction.

in local mechanical properties. Concerning numerical aspects, use has been made of the FFTW package (<http://www.fftw.org>) developed by Frigo and Johnson (2005). The computations have been performed on a mono-processor computer (2.33 GHz). The efficiency of our implementation has been tested for the same polycrystalline unit cell with different discretization grids. The discretization of the unit cell ranges from $N = 16^3$ to $N = 320^3$. The CPU time per elastic iteration is reported in Fig. 8. As expected, the computing time scales linearly with $N \log N$. It is noted that the chosen FFT package allows to get approximately the same scaling even when the number of voxels along each direction ($\sqrt[3]{N}$) is a prime number. For a local elastic anisotropy parameter $A = 2.8$, five FFT iterations are required in average to solve the problem with a relative error of 10^{-6} on the stress equilibrium condition. It is also interesting to consider the efficiency of the method in terms of memory size requirements. The size of a problem is characterized by the number of d.o.f. which is equal to $3N$. For illustration, the amount of memory required by our implementation of the full-field FFT modelling for $\sqrt[3]{N} = 128$ (~ 6 millions d.o.f) is 1 GB (compare with a recent study using FEM that required 21 GB of memory to solve a similar problem with less than 1 million d.o.f Houdaigui et al. (2007)).

References

- Bergman, D.J., 1978. The dielectric constant of a composite material – a problem in classical physics. *Phys. Rep.* 43, 377–407.
- Bobeth, M., Diener, G., 1987. Static and thermoelastic field fluctuations in multiphase composites. *J. Mech. Phys. Solids* 35, 137–149.
- Brenner, R., Castelnau, O., Badea, L., 2004. Mechanical field fluctuations in polycrystals estimated by homogenization techniques. *Proc. R. Soc. Lond. A* 460, 3589–3612.
- Budiansky, B., Hashin, Z., Sanders, J.L., 1960. The stress field of a slipped crystal and the early plastic behavior of polycrystalline materials. In: *Plasticity*, Proc. 2nd Symp. Naval Struct. Mech. Pergamon, Oxford, p. 239.
- Castelnau, O., Blackman, D.K., Lebensohn, R.A., Ponte Castañeda, P., 2008. Micromechanical modeling of the viscoplastic behavior of olivine. *J. Geophys. Res.* 113, B09202.
- Castelnau, O., Brenner, R., Lebensohn, R.A., 2006a. The effect of strain heterogeneity on the work hardening of polycrystals predicted by mean-field approaches. *Acta Mater.* 54, 2745–2756.
- Castelnau, O., Goudeau, P., Geandier, G., Tamura, N., Béchade, J., Bornert, M., Caldemaison, D., 2006b. White beam microdiffraction experiments for the determination of the local plastic behaviour of polycrystals. *Mater. Sci. Forum*, 103–108.
- Clausen, B., Lorentzen, T., Leffers, T., 1998. Self-consistent modelling of the plastic deformation of fcc polycrystals and its implications for diffraction measurements of internal stresses. *Acta Mater.* 46, 3087–3098.
- Eshelby, J.D., 1957. The determination of the elastic field of an ellipsoidal inclusion, and related problems. *Proc. R. Soc. Lond. A* 241, 376–396.
- Eyre, D.J., Milton, G.W., 1999. A fast numerical scheme for computing the response of composites using grid refinement. *J. Phys. III* 6, 41–47.
- Frigo, M., Johnson, S.G., 2005. The design and implementation of FFTW3. *Proceedings of the IEEE* 93 (2), 216–231. special issue on Program Generation, Optimization, and Platform Adaptation.
- Geandier, G., Gélébart, L., Castelnau, O., Bourhis, E.L., Renault, P.-O., Goudeau, P., Thiaudière, D., 2008. Micromechanical modeling of the elastic behavior of multilayer thin films; comparison with in situ data from X-ray diffraction. In: *IUTAM Book Series*. Springer.
- Hashimoto, K., Margolin, H., 1983a. The role of elastic interaction stresses on the onset of slip in polycrystalline alpha brass – I. Experimental determination of operating slip systems and qualitative analysis. *Acta Metall.* 31, 773–785.
- Hashimoto, K., Margolin, H., 1983b. The role of elastic interaction stresses on the onset of slip in polycrystalline alpha brass – II. Rationalization of slip behavior. *Acta Metall.* 31, 786–800.
- Hershey, A.V., 1954. The elasticity of an isotropic aggregate of anisotropic cubic crystals. *J. Appl. Mech.* 21, 236–240.
- Hill, R., 1952. The elastic behaviour of a crystalline aggregate. *Proc. Phys. Soc. A* 65, 349–354.
- Hill, R., 1963. Elastic properties of reinforced solids : some theoretical principles. *J. Mech. Phys. Solids* 11, 357–372.
- Hill, R., 1967. The essential structure of constitutive laws for metal composites and polycrystals. *J. Mech. Phys. Solids* 15, 79–95.
- Hook, R.E., Hirth, J., 1967. The deformation behavior of isoaxial bicrystals of Fe-3%Si. *Acta Metall.* 15, 535–551.
- Houdaigui, F.E., Forest, S., Gourgues, A.-F., Jeulin, D., 2007. On the size of the representative volume element for isotropic elastic polycrystalline copper. In: Bai, Y. (Ed.), *IUTAM Symposium on Mechanical Behavior and Micro-mechanics of Nanostructured Materials*. pp. 171–180.
- Hutchinson, J.W., 1970. Elastic-plastic behaviour of polycrystalline metals and composites. *Proc. R. Soc. Lond. A* 319, 247–272.
- Kreher, W., 1990. Residual stresses and stored elastic energy of composites and polycrystals. *J. Mech. Phys. Solids* 38, 115–128.
- Kröner, E., 1958. Berechnung der elastischen konstanten des vielkristalls aus den konstanten des einkristalls. *Z. Physik* 151, 504–518.
- Kröner, E., 1961. Zur plastischen verformung des vielkristalls. *Acta Metall. Mater.* 9, 155–191.
- Kröner, E., 1977. Bounds for effective elastic moduli of disordered materials. *J. Mech. Phys. Solids* 25, 137–156.
- Kröner, E., 1978. Self-consistent scheme and graded disorder in polycrystal elasticity. *J. Phys. F: Metal Phys.* 8, 2261–2267.
- Kumar, S., Kurtz, S.K., 1994. Simulation of material microstructure using a 3d voronoi tessellation: calculation of effective thermal expansion coefficient of polycrystalline materials. *Acta Metall. Mater.* 42, 3917–3927.
- Kumar, S., Kurtz, S.K., Agarwala, V.K., 1996. Micro-stress distribution within polycrystalline aggregate. *Acta Mech.* 114, 203–216.
- Lebensohn, R.A., 2001. N-site modeling of a 3D viscoplastic polycrystal using fast fourier transform. *Acta Mater.* 49, 2723–2737.
- Lebensohn, R.A., Liu, Y., Ponte Castañeda, P., 2004. On the accuracy of the self-consistent approximation for polycrystals: comparison with full-field numerical simulations. *Acta Mater.* 52, 5347–5361.
- Margolin, H., Wang, Z., Chen, T.-K., 1986. A model for yielding in anisotropic metals. *Metall. Trans. A* 17A, 107–114.
- Mehrabadi, M.M., Cowin, S.C., 1990. Eigentensors of linear anisotropic elastic materials. *Quart. J. Mech. Appl. Math.* 43, 15–41.
- Mendelson, K.S., 1981. Bulk modulus of a polycrystal. *J. Phys. D: Appl. Phys.* 14, 1307–1309.
- Meyers, M.A., Ashworth, E., 1982. A model for the effect of grain size on the yield stress of metals. *Philosophical Magazine* A 46, 737–759.
- Michel, J.C., Moulinec, H., Suquet, P., 2001. A computational scheme for linear and non-linear composites with arbitrary phase contrast. *Int. J. Numer. Meth. Engng.* 52, 139–160.
- Moulinec, H., Suquet, P., 1998. A numerical method for computing the overall response of nonlinear composites with complex microstructure. *Comput. Methods Appl. Mech. Engrg.* 157, 69–94.
- Moulinec, H., Suquet, P., 2003. Intraphase strain heterogeneity in nonlinear composites: a computational approach. *Eur. J. Mech. A/Solids* 22, 751–770.
- Nygards, M., 2003. Number of grains necessary to homogenize elastic materials with cubic symmetry. *Mech. Mater.* 35, 1049–1057.
- Nygards, M., Gudmundson, P., 2002. Three-dimensional periodic voronoi grain models and micromechanical fe-simulations of a two-phase steel. *Comput. Mater. Sci.* 24, 513–519.
- Pang, J., Holden, T., Turner, P., Mason, T., 1999. Intergranular stresses in zircaloy-2 with rod texture. *Acta Mater.* 47 (2), 373–383.
- Ponte Castañeda, P., Suquet, P., 1998. Nonlinear composites. *Adv. Appl. Mech.* 34, 171–302.
- Sab, K., 1992. On the homogenization and the simulation of random materials. *Eur. J. Mech. A/Solids* 11, 585–607.
- Sauzay, M., 2007. Cubic elasticity and stress distribution at the free surface of polycrystals. *Acta Mater.* 55, 1193–1202.
- Tamura, N., MacDowell, A., Spolenak, R., Valek, B., Bravman, J., Brown, W., Celestre, R., Padmore, H., Batterman, B., Patel, J., 2003. Scanning X-ray microdiffraction with submicrometer white beam for strain/stress and orientation mapping in thin films. *J. Synch. Rad.* 10, 137–143.
- Turner, P.A., Christodoulou, N., Tomé, C.N., 1995. Modeling the mechanical response of rolled zircaloy-2. *Int. J. Plasticity* 11, 251–265.
- Ungár, T., Castelnau, O., Ribárik, G., Drakopoulos, M., Béchade, J., Chauveau, T., Snigirev, A., Snigireva, I., Schroer, C., Bacroix, B., 2007. Grain to grain slip activity in plastically deformed zr determined by X-ray micro-diffraction line profile analysis. *Acta Mater.* 55, 1117–1127.
- Wikström, A., Nygards, M., 2002. Anisotropy and texture in thin copper films : an elastoplastic analysis. *Acta Mater.* 50, 857–870.
- Willis, J.R., 1977. Bounds and self-consistent estimates for the overall properties of anisotropic composites. *J. Mech. Phys. Solids* 25, 185–202.
- Yaguchi, M., Busso, E.P., 2005. On the accuracy of self-consistent elasticity formulations for directionally solidified polycrystal aggregates. *Int. J. Solids Struct.* 42, 1073–1089.
- Zeghadi, A., N'Guyen, F., Forest, S., Gourgues, A.-F., Bouaziz, O., 2007. Ensemble averaging stress-strain fields in polycrystalline aggregates with a constrained surface microstructure – part 1: anisotropic elastic behaviour. *Phil. Mag. A* 87, 1401–1424.
- Zeller, R., Dederichs, P.H., 1973. Elastic constants of polycrystals. *Phys. Status Solidi (b)* 55, 831–842.
- Zener, C., 1948. *Elasticity and Anelasticity of Metals*. University Chicago Press.